Multiplexed Modular Genetic Targeting of Quantum Dots

Saumya Saurabh,[†,‡] Lauren E. Beck,[‡,§] Suvrajit Maji,[‡,∥,⊗] Catherine J. Baty,[⊥] Yi Wang,[‡,#] Qi Yan,[‡,#,△] Simon C. Watkins,[⊥] and Marcel P. Bruchez[*,†,‡,∥,#]

[†]Department of Chemistry, [‡]Molecular Biosensor and Imaging Center, [§]Department of Physics, [∥]Lane Center for Computational Biology, and [#]Department of Biological Sciences, Carnegie Mellon University, Pittsburgh, Pennsylvania, United States and [⊥]Department of Cell Biology, Center for Biological Imaging, University of Pittsburgh, Pittsburgh, Pennsylvania, United States. [⊗]Present address: Department of Structural Biology, University of Pittsburgh School of Medicine, 2050 Biomedical Science Tower 3, 3501 Fifth Avenue, Pittsburgh, Pennsylvania 15260, United States. [△]Present address: Sharp Edge Laboratories, 2403 Sidney Street #264, Pittsburgh, Pennsylvania 15203, United States.

ABSTRACT While DNA-directed nanotechnology is now a well-established platform for bioinspired nanoscale assembly *in vitro*, the direct targeting of various nanomaterials in living biological systems remains a significant challenge. Hybrid biological systems with integrated and targeted nanomaterials may have interesting and exploitable properties, so methods for targeting various nanomaterials to precise biological locations are required. Fluorescence imaging has benefited from the use of nanoparticles with superior optical properties compared to fluorescent organic dyes or fluorescent proteins. While single-particle tracking (SPT) in living cells with genetically encoded proteins is limited to very short trajectories, the high photon output of genetically targeted and multiplexed quantum dots (QDs) would enable long-trajectory analysis of multiple proteins. However, challenges with genetic targeting of QDs limit their application in these experiments. In this report, we establish a modular method for targeting QD nanoparticles selectively to multiple genetically encoded tags by precomplexing QD—streptavidin conjugates with cognate biotinylated hapten molecules. This approach enables labeling and SPT of multiple genetically encoded proteins on living cells at high speed and can label expressed proteins in the cytosol upon microinjection into living cells. While we demonstrate labeling with three distinct QD conjugates, the approach can be extended to other specific hapten—affinity molecule interactions and alternative nanoparticles, enabling precise directed targeting of nanoparticles in living biological systems.

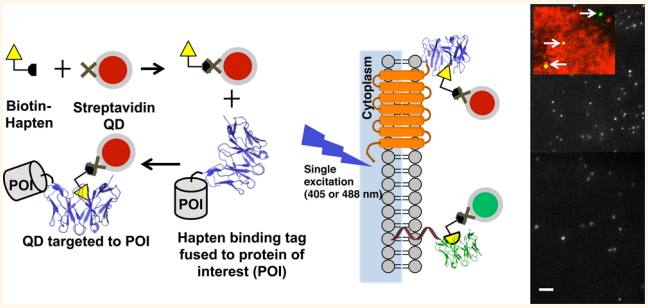

KEYWORDS: quantum dots · genetic targeting · membrane protein · single-molecule imaging

The use of nanotechnology tools for detecting or manipulating biological systems requires robust approaches to direct nanomaterials to biological targets. Developments in nanotechnology have led to nanoparticles of engineered size and shape in a variety of materials, including noble metals, insulators, semiconductors, magnetic materials, and composite structures available with a range of surface modifications and physical properties.[1−6] While gold and silicon nanoparticles have been primarily used for surface-enhanced Raman spectroscopy, electron microscopy, and magnetic resonance imaging, quantum dots (QDs) have been the nanoparticles of choice for fluorescence imaging[7−11] due to their excellent quantum yields, long-term photostability, and advantageous spectroscopic properties. For these properties to be exploited for biological objectives, the nanoparticles should be precisely located at sites of biological interest in or inside live and fixed cells. The conventional labeling approach has delivered a variety of nanoparticles to live cells using antibody, peptide, DNA, and aptamer conjugates, but requires molecules with robust affinity for a specific target.[12−14] In contrast, genetically encoded epitope tags[15] and fluorescent proteins[16] have been fused to nearly every eukaryotic protein, allowing detection of each target in a cellular context. The power of genetic targeting arises from the resulting protein-level fusion, carrying the tag where the target is directed by the cell. The development of orthogonal and modular genetic targeting approaches is required to effectively exploit the properties of nanomaterials in biological systems.

* Address correspondence to bruchez@cmu.edu.

Received for review March 13, 2014 and accepted November 7, 2014.

Published online November 07, 2014
10.1021/nn5044367

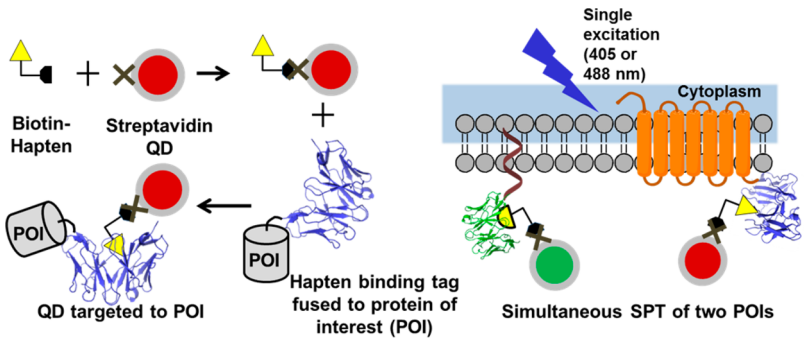

Figure 1. Genetic targeting of sav-QDs using biotinylated haptens that bind to genetically encoded tags fused to proteins of interest. The method can be utilized for simultaneous single-particle tracking (SPT) of multiple proteins of interest in the cell surface using a single excitation source.

Since the first demonstrations of bioconjugated QDs, several approaches at the interface of nanotechnology and biology have led to an increase in the use of QDs for live cell imaging.[10,11] QDs have been used extensively for labeling and imaging cellular proteins particularly at the single-molecule level.[17,18] Their brightness, photostability, and multicolor properties make single-molecule imaging possible at very high speeds and low exposures, thus improving temporal resolution.[19] Traditionally, QDs have been targeted to proteins of interest as antibody or biomolecule conjugates, resulting in a typically multivalent probe that may interfere with protein function.[20−22] There have been several efforts to target QDs using smaller affinity tags. QDs functionalized with fluorescein were used to target a mouse prion protein fused to an antifluorescein scFv.[23,24] Another approach showed the tracking of single poly-histidine-tagged proteins using QDs functionalized with Ni^{2+} tris-nitrilotriacetic acid.[25,26] More recently, QDs functionalized with haloTag protein were used to target single LDL receptor proteins on the cell surface that had been previously tagged using a lipoic acid ligase directed 10-bromodecanoate substrate.[27,28] Similar methods have been used in conjunction with biotin or other small-molecule tags to target streptavidin (sav)-functionalized QDs after biotin modification of the proteins.[29] While these approaches enabled targeting of QDs to cell surface proteins, their general application is limited by the synthetic steps required to prepare the functionalized QDs. In addition, the postlabeling approach is not easy to implement for multiplexing. The shared excitation and narrow emission spectra of QDs can be exploited for simultaneous multiplexing, but lacking robust orthogonal targeting approaches, multiplex labeling has been limited to complex prelabeling procedures (*i.e.*, biotin ligase and lipoic acid ligase treatment), multicolor labeling of a single target, or antibody precomplexation.[30,31] Here we report a technique to target commercially available sav-QDs (consisting of a CdSe/CdTe core and a ZnS shell, with 5−10 sav per QD) using biotinylated hapten molecules that specifically bind to small genetically encoded proteins with high affinities. The schematic for the targeting method is shown in Figure 1. Due to the high affinity and fast on-rate of the hapten−protein complex formation, the labeling is instantaneous and requires only one washing step before imaging. The large number of available haptens with specific cognate proteins provides a highly modular labeling scheme, potentially limited only by the number of resolvable detection channels. We show that this method can achieve orthogonal labeling for at least three targets on the surface of cells, can label multiple cell surface proteins for simultaneous single-molecule tracking at high speeds and over long time scales, and can be applied to target sav-QDs to intracellular proteins. We also demonstrate that despite the multivalency of the sav-QDs, it is the hapten ratio that ensures monovalency in binding to the scFvs. The QDs, due to the ease of multiplexed detection, serve as a robust targeting model for various nanoparticles, demonstrating that this approach can specifically target three or more different nanoparticles to genetically specified locations, as long as those nanoparticles are available as biotin-binding conjugates.

RESULTS AND DISCUSSION

A robust genetically encoded targeting approach must be both specific and selective for the expressed protein tag. Single-chain variable fragment (scFv) antibodies with molecular recognition properties for fluorescent and fluorogenic dye haptens have been established with dissociation constants (K_d) ranging from low nanomolar to picomolar ranges and corresponding dissociation times of several hours.[30,32,33] In this study, we demonstrate that biotinylated analogues of these dye-based haptens can target commercially available sav-QD conjugates to the cognate genetically encoded binding protein. The chemical structures of the dye-based haptens are shown in Figure 2. JAR200 yeast cells carrying a gene for expressing cell-wall-anchored protein dL5** that binds to Malachite Green (MG) (K_d = 18 pM, k_{off} = 1.5 × 10^{-4} s^{-1}) were selectively labeled with sav-QDs of all available colors (QD525, QD565,

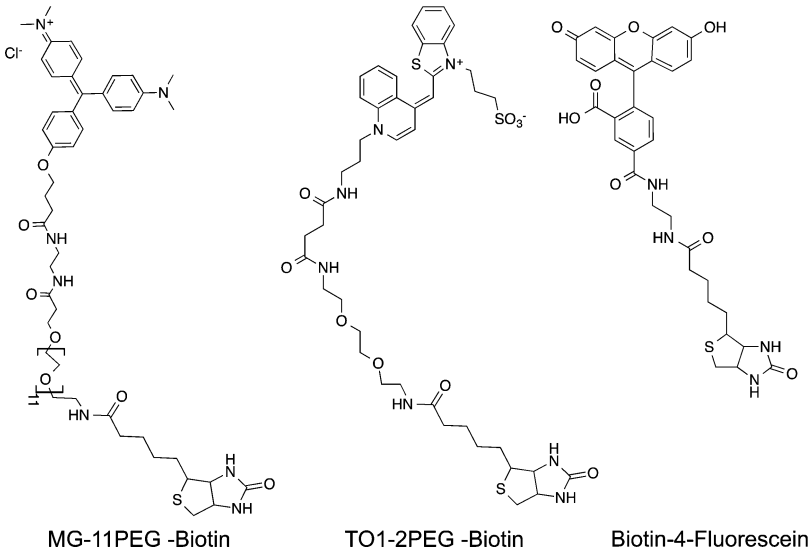

Figure 2. Chemical structures of biotin-haptens used in this study. MG-11PEG-biotin binds dL5, TO1-2PEG-biotin binds HL1.0.1, and biotin-4-fluorescein binds E2. The syntheses of MG-11PEG-biotin and TO1-2PEG-biotin are outlined in ref 32. Biotin-4-fluorescein was obtained commercially from Sigma-Aldrich.**

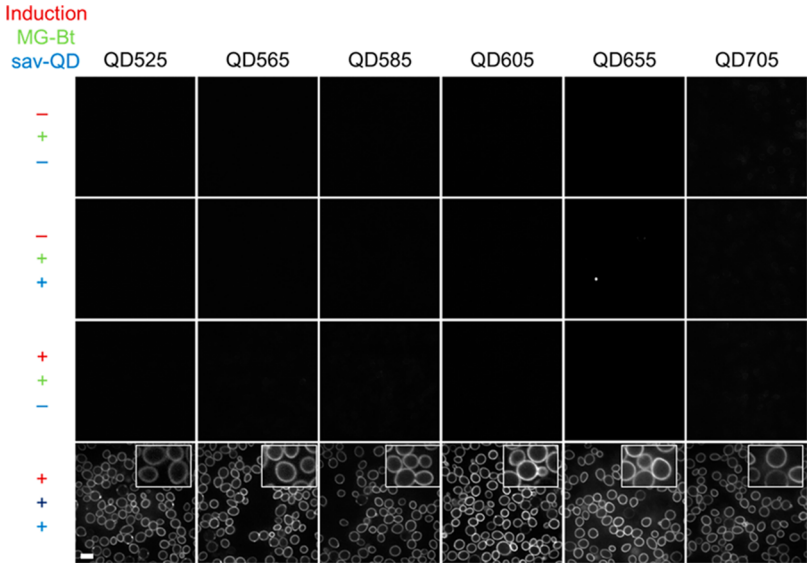

Figure 3. JAR200 cells containing a dL5 plasmid in a pPNL6 vector were grown (top two rows) and imaged after incubation with MG-Bt only and MG-QD conjugate. Due to the absence of dL5** protein, QDs are not targeted to the cell surface. Induced JAR200 cells (bottom two rows) that expressed dL5** protein on their surface were imaged only when the MG-QD conjugate is present under 405 nm excitation. Shown in the inset are zoomed-in views of regions within the sample showing very uniform labeling of the cell surface proteins using this approach. The imaging was performed using an inverted epi-fluorescence microscope. The emission filters used for each QD were centered at the QD emission peak and had a 20 nm bandwidth; scale bar 15 μm.**

QD585, QD605, QD655, QD705) only when induced to express the hapten-binding protein and preincubated with MG-biotin (MG-Bt), as shown in Figure 3.[34] We can see from the zoomed images of labeled cells that the QD labeling is very uniform on the cell surface. Prebinding of biotinylated hapten to sav-QD conjugates can also selectively label cognate protein tags on cells. scFvs that bind to MG (dL5**), a sulfonated thiazole orange (TO1) analogue (HL1.0.1) (K_d = 1.7 nM), and fluorescein (E2) (K_d = 1.1 nM, $k_{off} = 4.4 \times 10^{-3}$ s^{-1}) were expressed on the yeast cell wall as above.[32,33,35] sav-QD655 was preincubated with saturating amounts of the respective biotinylated hapten, separated from excess hapten, and then incubated with JAR200 cells expressing each protein. Imaging of the cells revealed that the QD−hapten complex labels only the cognate protein for the bound hapten, demonstrating the modularity and orthogonality of the labeling strategy with three distinct hapten-scFv pairs, MG-dL5**, TO1-HL1.0.1, and Fl-E2 (Figure 4A). Additionally, a mixed population of JAR200 cells expressing HL1.0.1, E2-FITC, or dL5** were labeled with TO1-QD565, Fl-QD605, and MG-QD655, respectively, using the same protocols as above. These cells were imaged using a 405 nm laser excitation and suitable band-pass

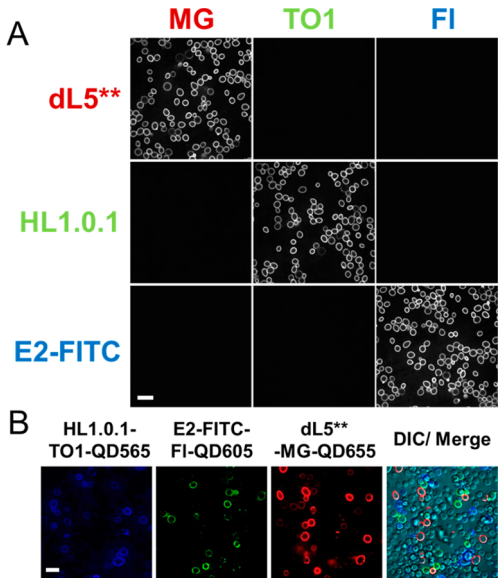

Figure 4. (A) Precomplexation of the QDs and haptens allows selective targeting of QDs to cognate expressed scFvs. The targeting is specific, and QD signal is only observed when the QDs are bound to the correct hapten for the cognate protein. Here, dL5 binds MG, HL1.0.1 binds TO1, and E2-FITC binds fluorescein (FI). No labeling is seen with any noncognate pairs. The cells were incubated with QD-hapten solutions followed by washing and plating in imaging dishes. Imaging was performed using an inverted epi-fluorescence microscope with 488 nm excitation and a 655/20 nm emission filter. (B) Three-color multiplexing experiment on the surface of three different strains of JAR200 yeast cells expressing HL1.0.1, E2-FITC, and dL5**. The cells were imaged as in (A), but using 565/20 nm (blue), 610/40 nm (green), and 685/70 nm (red) emission filters; scale bar 20 μm.**

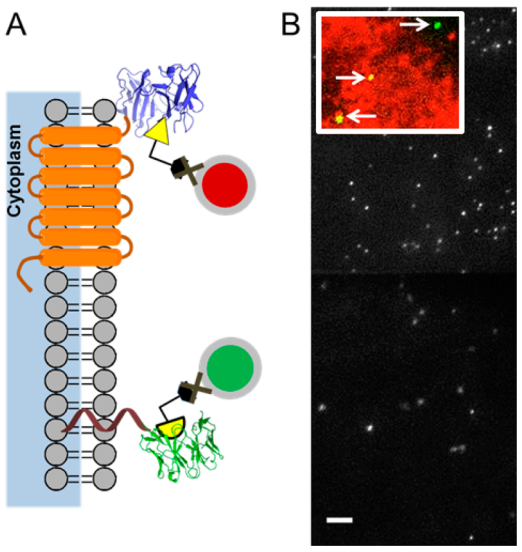

Figure 5. (A) Schematic showing dL5-B2AR fusion on the cell membrane bound to MG-QD655 and a TM-HL1.0.1 bound to TO1-QD605. (B) Single-molecule images acquired using a TIRF microscope equipped with a dual-view splitter showing the B2AR molecules labeled with QD655 (top) and the HL1.0.1-TM molecules labeled with QD605. Once the QDs are bound, the remaining receptors can be saturated with the fluorogenic hapten (MG) to perform ensemble imaging using the fluorescence from dL5**-MG (ex 640 nm, em 685/70 nm, red signal) and single-molecule imaging using QD605 (ex 405 nm, em 605/20 nm, green dots marked with arrows) simultaneously (5B, inset); scale bar 1 μm.**

filters for detection. Induced yeast cells typically have a nonexpressing population, visible as unstained cells in the DIC overlay. These results demonstrate the multiplexing of three different colored QDs in the same experiment using a simple mix-and-label protocol (Figure 4B). Thus, these protein−hapten pairs are suitable for simultaneous multicolor use since the expressed protein tags recognize only one dye. Purified dL5** assembled with MG-QDs of different colors showed no sign of energy transfer to the surface-bound MG protein complex (supplementary Figure 1). The imaging of different colored QDs using our methodology is achievable by a careful selection of emission filters and is only limited by the availability of the cognate scFv-hapten pairs in a given study.[3,30,36]

Due to the high affinity and slow dissociation rate of the hapten−scFv complexes, targeted QDs are retained sufficiently for simultaneous multiplexed imaging and single-particle tracking. A HEK293 cell line with stable expression of dL5**-β-2-adrenergic receptor (B2AR) fusion (methods) was transfected to express HL1.0.1 on the cell surface anchored by a single-platelet-derived growth factor receptor transmembrane domain (TM) from the pDisplay vector.[37] MG-Bt and TO1-Bt were incubated with sav-QD655 and sav-QD605, respectively, to form MG-QD655 and TO1-QD605 complexes (1:8 QD:hapten).[32] These QD-hapten complexes were then added to a glass-bottom imaging dish containing the HEK293 cells and then washed to remove unbound QDs. Microscopy was performed at the basal surface of the cells at 37 °C, using total internal reflection fluorescence (TIRF) illumination with a dual-view image splitter to simultaneously image QD605 and QD655 under a 405 or 488 nm excitation at 40 Hz and 25 ms exposure. The protein labeling schematic is shown in Figure 5A. The images from this experiment are shown in Figure 5B and supplementary movie S1. After labeling a sparse subset of receptors with MG-QD605 complex, addition of the MG fluorogen to the media labeled the remaining scFv sites, showing spectrally resolvable ensemble and single-molecule imaging.[32] Using the 640 nm laser, we could selectively excite the dL5**-MG complex, while the 405 nm laser excited bound QD605, as shown in Figure 5B (inset). It should be noted that the excitation of QD655 at this wavelength is only 18% of its excitation at 405 nm. Additionally the QDs are at a single-molecule density, while the dL5**-MG complexes are at an ensemble density. These two facts enable the simultaneous ensemble and single-molecule labeling shown here.[32]

We performed single-particle tracking to determine diffusion coefficients of these proteins on the cell

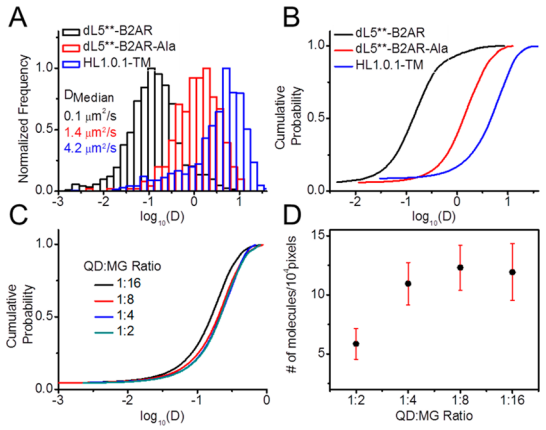

Figure 6. (A) Distribution of coefficients of the dL5-B2AR, dL5**-B2AR-Ala, and HL1.0.1-TM on the surface of HEK293 cells. The TM protein displays a ~40× larger diffusion coefficient than the B2AR measured simultaneously on the same cells. The B2AR-Ala molecules have diffusion coefficients significantly larger than WT B2AR molecules owing to the lack of interactions with the PDZ domain. (B) Cumulative distribution functions for the diffusion coefficients of the samples in (A) are shown. (C) CDFs and (D) number of molecules in a 100 by 100 pixel region for dL5**-B2AR diffusion measurements at different occupancy ratios of QD:MG. While a ratio of 1:16 produces slower diffusion, a ratio of 1:2 gives a lower molecular density. For the diffusion coefficients in (A) we are away from both the extremes at a ratio of 1:8.**

surface using mean-squared displacement analysis for each particle trajectory.[38,39] Mean trajectory lengths for B2AR and TM-HL1.0.1 were 19 and 13 frames, respectively ($N > 600$ tracks, see Methods), when no attempts were made to link trajectories due to blinking or diffusion out of the image plane. These trajectories are suitable for mean-squared displacement (MSD) analyses using standard methods.[40] We used these analyses to calculate the diffusion coefficients for the membrane proteins. While the B2AR shows slow diffusion over short ranges, the TM protein diffuses rapidly over long ranges (Figure 6A). We found the median diffusion coefficient (D) of the HL1.0.1-TM protein to be 4.2 $\mu m^2/s$, while the B2AR protein measured on the same cells, under the same conditions, diffuses with a D of 0.1 $\mu m^2/s$ (Figure 6A). These results are consistent with previous reported diffusion coefficients of B2AR and TM constructs in HEK293 cells.[41] Self-consistent median D values of 4.5 $\mu m^2/s$ (HL1.0.1-TM) and 0.1 $\mu m^2/s$ (dL5**-B2AR) were obtained for these labeled proteins, respectively, when the labeling colors were transposed (MG-QD605:B2AR/TO1-QD655:TM-HL1.0.1), indicating that the protein target, not the scFv-QD complex, is responsible for the observed differences in diffusion. Additionally, these results are in agreement with previous results on membrane proteins with QDs, indicating that the observed effect is solely due to the proteins and not the QDs.[42]

The endocytic sorting of the B2AR is controlled by its interaction with a kinase-regulated PDZ domain.[43] An alanine (Ala) mutation at the carboxy-terminus of the B2AR suppresses its interactions with the PDZ domain. HEK293 cells were transfected with a dL5**-B2AR-Ala plasmid. The dL5** protein was labeled using MG-QD655, and single-molecule imaging was performed as above. These B2AR-Ala mutant proteins diffused rapidly at a rate of 1.4 $\mu m^2/s$ (Figure 6A and supplementary movie S2). These results are also consistent with previous studies.[44] Cumulative distribution functions (CDF) of the diffusion coefficients for dL5**-B2AR, dL5**-B2AR-Ala, and HL1.0.1-TM were calculated (Figure 6B).

The stoichiometry of QD:hapten used for yeast cell imaging and single-molecule experiments was 1:8. We further asked if this ratio has an impact on the QD−hapten binding to the protein on the cell surface and/or their diffusion. For this, we used four different ratios of QD655 and MG-Bt (1:2, 1:4, 1:8, and 1:16) to perform single-molecule trajectory analysis of the dL5**-B2AR protein. At the highest hapten loading QD:MG ratio (1:16) used, we observed a very pronounced 2-fold decrease in the median diffusion coefficient, suggesting that the occupancy of QD and the number of binding sites can play a role in its diffusion (Figure 6C). The diffusion behavior for lower loading is invariant as we go from 1:8 to 1:2 in QD:hapten stoichiometry. However, we see that for the lowest loading used (1:2), the labeling density is significantly lower than for higher loading ratios (Figure 6D). These results indicate that a low density of haptens reduces labeling of targets, while a high density of haptens can alter diffusion, potentially due to cross-linking or clustering receptors. This can be titrated without risks of QD aggregation due to the monovalent biotin−hapten reagents and their association with univalent scFv proteins. We would like to emphasize that for any particular cell labeling, these titrations must be performed to find out the optimum QD:hapten occupancy ratio in order to obtain optimal labeling density while minimally perturbing the diffusion of proteins of interest. Importantly, this labeling method affords a very straightforward approach to test single-particle tracking experiments for valency associated artifacts.

In order to confirm that QD-hapten binding to mammalian cells was specific, we incubated QD655 with HEK293 cells expressing dL5**-B2AR on the cell surface. We observed very rapid movement of the QDs with a high background. Upon washing three times with imaging media, however, few QDs were retained on the cell surface (supplementary movie S3 and supplementary Figure 2). Additionally, incubating MG-QD655 with WT HEK293 cells also showed rapidly moving particles that were not retained upon washing the cells three times with the imaging media (supplementary movie S4). Given that cell imaging was performed after washing the cells 3×, the observed signals are due to the specific binding of the hapten-QDs to the membrane proteins on the cell surface, rather than nonspecifically trapped or bound QD particles.

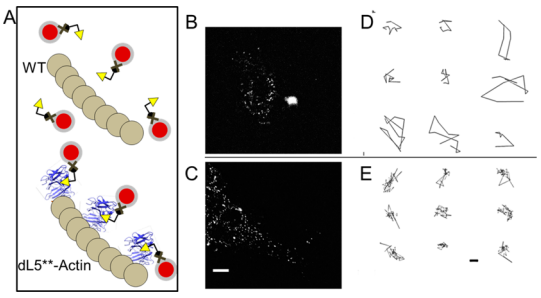

Figure 7. (A) Schematic of MG-QD in the cytoskeleton showing that the QDs are targeted to the protein of interest (actin) only when the cognate protein for the hapten (dL5) is present, and otherwise show free diffusion in the cytosol. MG-QD655 injected in HeLa cells (B) and injected in HeLa cells expressing dL5**-actin (C); scale bar 4 μm. The bright spot in (B) is the spot where the MG-QD655 was injected in the cell. (D) and (E) show single-molecule trajectories for QD-MG complexes in wild-type and dL5**-actin-expressing HeLa cells; scale bar 100 nm.**

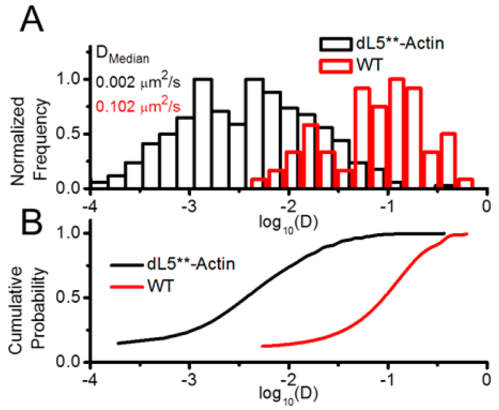

Figure 8. (A) Distribution of diffusion coefficients of the MG-QD655 in WT HeLa cells and HeLa cells expressing dL5-actin labeled with MG-QD655. (B) Cumulative distribution functions for the diffusion coefficients of the samples in (A) are shown.**

The delivery of a small number of QDs inside the cells is very advantageous since it can enable single-molecule studies of QD conjugates using a conventional epi-fluorescence setup. The injection of well-dispersed, single MG-QD655 using a modified microinjection protocol in WT HeLa cells showed single particles with significant diffusion (Figure 7A and B), while injection into HeLa cells stably expressing dL5**-actin (Figure 7A and C) showed rapid immobilization of injected QDs. Representative single-molecule trajectories from these two experiments are also shown (Figure 7D and E). While trajectories from dL5**-actin-expressing cells span 100–500 nm, the WT trajectories span a much larger distance, implying that the QDs are bound to dL5**-actin post-microinjection. These results are also shown in supplementary movie S5. Diffusion coefficients for MG-QDs bound to dL5**-actin were essentially negligible (D = 0.002 μm^2/s), whereas free MG-QDs in WT cells showed significant diffusion at a rate of 0.102 μm^2/s, which is in agreement with the reported diffusion properties of other free QDs in the cytoplasm.[45] The distributions of diffusion coefficients for dL5**-actin labeled with MG-QD655 and MG-QD655 in nontransfected cells are shown in Figure 8A, and the CDFs are shown in Figure 8B. The marked difference between MG-QD complex diffusion in WT and dL5**-actin-expressing cells indicates that the MG-QDs can be targeted to dL5**-actin, and potentially other targets, inside HeLa cells when delivered into the cell through microinjection.

CONCLUSIONS

Here we have demonstrated a general genetic targeting and multiplexing approach using commercially available sav-QDs that is useful for specific and multiplexed labeling of genetically encoded tags. We have shown that the targeting using scFv-hapten complexes is specific and depends only on the scFv-hapten pair used. We have established a method for studying two different proteins on the cell surface simultaneously at high speeds (40 FPS) and low exposure times (25 ms), which can be further improved by using faster cameras and methods to spectrally separate fluorescence into more channels. In addition, we have delivered the MG-QD complexes into live cells for detection of single actin proteins in the cytoskeleton.

The immense selectivity of antibodies and a large structural diversity of haptens suggest that this method may be substantially extended beyond the three orthogonal targets demonstrated here. scFv proteins that recognize various dye molecules, peptides, and drug-based haptens have been demonstrated with subnanomolar affinities.[32,33] Preparation of biotinylated analogues of these haptens is often required during the selection process or readily achievable with simple chemical modification, and streptavidin conjugates of various nanoparticles are typically among the first bioconjugates prepared.[36] Together, these facts suggest that this approach could be rapidly expanded to new protein–hapten pairs and new particle chemistries for multiplexed imaging in biophysics and cell biology. High-affinity intracellular protein–ligand complexes (*e.g.*, the trimethoprim-eDHFR complex TMP-tag) may improve the approach for intracellular detection when combined with methods or chemistries that improve delivery of QDs into cells.[45–48]

METHODS

Yeast Cell Labeling Using QD-Haptens. For yeast cell imaging, all strains (JAR200) expressing the respective proteins on the surface (pPNL6 expression vector) were grown in 3 mL of growth media (20 g of dextrose, 5 g of casamino acids, 1.7 g of yeast nitrogen base, 5.3 g of ammonium sulfate, 7.4 g of

sodium citrate, 2.2 g of citric acid per liter at pH 4) at 30 °C for 24 h.[32,33] A 0.7 mL amount of yeast cells from the culture was induced in 35 mL of SG/R-CAA (1 g of dextrose, 20 g of raffinose, 20 g of galactose, 5 g of casamino acids, 1.7 g of yeast nitrogen base, 5.3 g of ammonium sulfate, 60 mg of uracil per liter at pH 7.4) at 20 °C for 72 h. One milliliter of this culture was spun down, and media was removed. Cells were then washed 3× with 1 mL of PBS and incubated at 4 °C for 2 h in 100 μL of PBS with 1 μM biotin-hapten. Unbound hapten was then removed, and cells were washed 2× with 1 mL of PBS. Cells were then incubated at 4 °C for 30 min in 20 μL of PBS with 50 nM sav-QD (Life Technologies, Inc.). Unbound QD was then removed, and cells were washed 1× with 1 mL of PBS. Cells were then resuspended in 100 μL of PBS.

Precomplexation Approach Using QD-Haptens. sav-QD (5 nM) and biotin-hapten (40 nM) were incubated at 4 °C in 1 mL of PBS for 30 min. The complex was then centrifuged in a 10 000 MWCO spin filter (Microcon YM10) to remove unbound fluorogen. The retained complex was then added to cells and incubated as above. A 20 μL portion of the resuspended cells was then imaged in 2 mL of PBS on glass bottom dishes (MatTek Corp.) coated with concanavalin A.

Yeast Cell Imaging. Imaging was performed on an epi-fluorescence microscope (Nikon Ti Eclipse inverted microscope), using a planApo-chromat objective (60×, 1.45 N.A., Nikon). The samples were excited using DPSS lasers at 405 and 488 nm through a filter cube consisting of a quad band excitation filter (405, 488, 532, and 640 nm), a quad band dichroic filter, and a 505 long-pass emission filter (all from Chroma Technology). We used an additional emission filter for each QD such that the filter was a 20 nm band-pass centered at the nominal QD emission peak, except for the 705 QDs that used a 680 nm long-pass filter. Images were acquired using an EMCCD camera (iXon DV897, Andor Technologies) with an EM gain of 250 and an exposure time of 50 ms. For the multiplexing experiment in Figure 4B, we used an excitation laser at 405 nm and the emission filters 565/20, 610/40, and 685/70. We do observe ∼10% cross talk of QD565 and QD655 into the 610/40 nm filter, which is expected with this filter set, based on the spectral properties of these QDs.

Plasmid and Mammalian Cell Line Preparation. pBabe-dL5**-B2AR was generated by inserting the dL5 sequence into pBabeSac-ADRB2Lac2 using SfiI cutting sites. Stable HEK293 cells were generated by transfecting HEK293 cells with pBabe-dL5**-β2-AR followed by drug selection (1 mg/mL puromycin, Invitrogen) and FACS enrichment (Becton Dickinson FACS Vantage flow cytometer; excitation 633 nm, emission 685/35 nm).

Mammalian Cell Surface Protein Imaging. For mammalian cell imaging, a stable HEK293 cell line expressing B2AR-dL5** chimera was transfected with HL1.0.1-PDGFR-TM plasmid DNA [3] using Lipofectamine 2000 transfection reagent (Life Technologies) as per the manufacturer's guidelines. Imaging was performed on the same system as above, utilizing 405 nm excitation in the total internal reflection (TIR) mode. The microscope was equipped with a TIRF objective (100×, 1.49 NA, Nikon) dual-view DV2 splitter (Photometrics) consisting of a 625 nm dichroic and two band-pass filters (605/20 and 655/20, Chroma Technology). TO1-QD605 and MG-QD655 were used to label HL1.0.1-TM and dL5**, respectively. Images were acquired using the same EMCCD camera as above at an exposure time of 25 ms. Single-particle tracking and mean-squared displacement analyses were performed using particle tracking code written in Matlab. For MSD analyses, no attempts were made to reconnect broken trajectories. As a result, for dense data sets such as movie S1, the mean trajectory length was 18 frames compared to sparse data sets such as movie S2, where the mean was 443 frames.

Mammalian Cell Intracellular Imaging. For imaging QDs inside the cells, microinjection was performed in a HeLa cell line that expressed dL5** on actin. As a control, a HeLa cell line without the dL5** was used. Live cell imaging was done in a system with a motorized stage, on a Nikon Ti Eclipse inverted fluorescent microscope equipped with a 60× plan apo lens (Nikon Inc.), fluorescent illuminator (89 North, Burlington, VT, USA), CoolSNAP HQ2 camera (Photometrics), and NIS Elements 4.2. QD imaging was done using an EGFP long-pass filter cube (Chroma, C49012) with emission optimized for QDs (either 685/70 or 585/20). Confocal swept-field imaging was done using the same microscope platform and Andor DU-897 camera. Microinjection used Femtojet, Inject Man Ni 2, and Femtotips II (all by Eppendorf) . We successfully minimized issues of needle clogging by manual needle tip enlargement with brief contact with a cotton ball as suggested in Sutter Pipette Cookbook (Sutter Instrument Co., Novato, CA, USA). Tracking and MSD analyses were done as described above.

Filter Specifications. Throughout the article, the specification of the filters as XXX/YY implies that wavelengths ranging from XXX−(YY/2) to XXX+(YY/2) can pass through the filter.

A Note on the Number of Streptavidin Molecules per QD. The manufacturer's specification sheet mentions that there are 5−10 streptavidin molecules per QD. However, in order to characterize the exact number of streptavidin molecules per QD, a biotin-4-fluorescein quenching based technique can be used.[49]

Conflict of Interest: The authors declare the following competing financial interest(s): M.P.B. is a founder and Q.Y. is a current employee of Sharp Edge Labs, a company commercializing assays based on fluorogen-activating peptides.

Supporting Information Available: Supplementary Figures 1 and 2 and movies S1 through S5. This material is available free of charge *via* the Internet at http://pubs.acs.org.

Acknowledgment. This research was funded through NIH grant U54GM103529, Astrid and Bruce McWilliams fellowship (S.S.), and R01GM100114 (M.P.B.). We thank Dr. Cheryl Telmer (CMU) for providing us with the HL1.0.1 plasmid for transfections and Prof. Cheemeng Tan (UC Davis) for a critical reading of the manuscript. The research and experimental design was conceived by S.S. and M.P.B. Experiments were performed by S.S., L.E.B., Y.W., and C.J.B. SPT analysis was performed by S.S. and S.M. Stable HEK cell lines expressing dL5**-B2AR and the B2AR-Ala constructs were prepared by Q.Y. Materials and reagents were provided by M.P.B. and S.C.W. Results were interpreted and the manuscript was written by S.S. and M.P.B. with inputs from S.M. and C.J.B.

REFERENCES AND NOTES

1. Daniel, M.-C.; Astruc, D. Gold Nanoparticles: Assembly, Supramolecular Chemistry, Quantum-Size-Related Properties, and Applications toward Biology, Catalysis, And Nanotechnology. *Chem. Rev.* **2004**, *104*, 293–346.
2. Li, Z.; Barnes, J. C.; Bosoy, A.; Stoddart, J. F.; Zink, J. I. Mesoporous Silica Nanoparticles in Biomedical Applications. *Chem. Soc. Rev.* **2012**, *41*, 2590–2605.
3. Goldman, E. R.; Clapp, A. R.; Anderson, G. P.; Uyeda, H. T.; Mauro, J. M.; Medintz, I. L.; Mattoussi, H. Multiplexed Toxin Analysis Using Four Colors of Quantum Dot Fluororeagents. *Anal. Chem.* **2003**, *76*, 684–688.
4. Laurent, S.; Forge, D.; Port, M.; Roch, A.; Robic, C.; Vander Elst, L.; Muller, R. N. Magnetic Iron Oxide Nanoparticles: Synthesis, Stabilization, Vectorization, Physicochemical Characterizations, and Biological Applications. *Chem. Rev.* **2008**, *108*, 2064–2110.
5. Akerman, M. E.; Chan, W. C. W.; Laakkonen, P.; Bhatia, S. N.; Ruoslahti, E. Nanocrystal Targeting in Vivo. *Proc. Natl. Acad. Sci. U.S.A.* **2002**, *99*, 12617–12621.
6. Sapsford, K. E.; Algar, W. R.; Berti, L.; Gemmill, K. B.; Casey, B. J.; Oh, E.; Stewart, M. H.; Medintz, I. L. Functionalizing Nanoparticles with Biological Molecules: Developing Chemistries that Facilitate Nanotechnology. *Chem. Rev.* **2013**, *113*, 1904–2074.
7. Yigit, M. V.; Medarova, Z. In Vivo and ex Vivo Applications of Gold Nanoparticles for Biomedical SERS Imaging. *Am. J. Nucl. Med. Mol. Imaging* **2012**, *2*, 232–241.
8. Margus, H.; Padari, K. r.; Pooga, M. Insights Into Cell Entry and Intracellular Trafficking of Peptide and Protein Drugs Provided by Electron Microscopy. *Adv. Drug Delivery Rev.* **2013**, *65*, 1031–1038.
9. Kairdolf, B. A.; Smith, A. M.; Stokes, T. H.; Wang, M. D.; Young, A. N.; Nie, S. Semiconductor Quantum Dots for

Bioimaging and Biodiagnostic Applications. *Annu. Rev. Anal. Chem.* **2013**, *6*, 143–162.
10. Nagy, A.; Gemmill, K. B.; Delehanty, J. B.; Medintz, I. L.; Sapsford, K. E. Peptide-Functionalized Quantum Dot Biosensors. *IEEE J. Sel. Top. Quantum Electron.* **2014**, *20*, 115–126.
11. Lane, L. A.; Smith, A. M.; Lian, T.; Nie, S. Compact and Blinking-Suppressed Quantum Dots for Single-Particle Tracking in Live Cells. *J. Phys. Chem. B* **2014**. DOI: 10.1021/jp5064325.
12. Chen, F.; Gerion, D. Fluorescent CdSe/ZnS Nanocrystal-Peptide Conjugates for Long-Term, Nontoxic Imaging and Nuclear Targeting in Living Cells. *Nano Lett.* **2004**, *4*, 1827–1832.
13. Tan, W.; Donovan, M. J.; Jiang, J. Aptamers from Cell-Based Selection for Bioanalytical Applications. *Chem. Rev.* **2013**, *113*, 2842–2862.
14. Penn, S. G.; He, L.; Natan, M. J. Nanoparticles for Bioanalysis. *Curr. Opin. Chem. Biol.* **2003**, *7*, 609–615.
15. Yang, X.; Boehm, J. S.; Yang, X.; Salehi-Ashtiani, K.; Hao, T.; Shen, Y.; Lubonja, R.; Thomas, S. R.; Alkan, O.; Bhimdi, T.; *et al.* A Public Genome-Scale Lentiviral Expression Library of Human Orfs. *Nat. Methods* **2011**, *8*, 659–661.
16. Howson, R.; Huh, W. K.; Ghaemmaghami, S.; Falvo, J. V.; Bower, K.; Belle, A.; Dephoure, N.; Wykoff, D. D.; Weissman, J. S.; O'Shea, E. K. Construction, Verification And Experimental Use of Two Epitope-Tagged Collections of Budding Yeast Strains. *Comp. Funct. Genomics* **2005**, *6*, 2–16.
17. Bruchez, M. P. Quantum Dots Find their Stride in Single Molecule Tracking. *Curr. Opin. Chem. Biol.* **2011**, *15*, 775–780.
18. Pinaud, F.; Clarke, S.; Sittner, A.; Dahan, M. Probing Cellular Events, One Quantum Dot at a Time. *Nat. Methods* **2010**, *7*, 275–285.
19. Michalet, X.; Pinaud, F. F.; Bentolila, L. A.; Tsay, J. M.; Doose, S.; Li, J. J.; Sundaresan, G.; Wu, A. M.; Gambhir, S. S.; Weiss, S. Quantum Dots for Live Cells, in Vivo Imaging, and Diagnostics. *Science* **2005**, *307*, 538–544.
20. Dahan, M.; Lévi, S.; Luccardini, C.; Rostaing, P.; Riveau, B.; Triller, A. Diffusion Dynamics of Glycine Receptors Revealed by Single-Quantum Dot Tracking. *Science* **2003**, *302*, 442–445.
21. Bhattacharyya, S.; Bhattacharya, R.; Curley, S.; McNiven, M. A.; Mukherjee, P. Nanoconjugation Modulates the Trafficking and Mechanism of Antibody Induced Receptor Endocytosis. *Proc. Natl. Acad. Sci. U.S.A.* **2010**, *107*, 14541–14546.
22. Tekle, C.; Deurs, B. v.; Sandvig, K.; Iversen, T.-G. Cellular Trafficking of Quantum Dot-Ligand Bioconjugates and Their Induction of Changes in Normal Routing of Unconjugated Ligands. *Nano Lett.* **2008**, *8*, 1858–1865.
23. Biju, V.; Itoh, T.; Ishikawa, M. Delivering Quantum Dots to Cells: Bioconjugated Quantum Dots for Targeted And Nonspecific Extracellular and Intracellular Imaging. *Chem. Soc. Rev.* **2010**, *39*, 3031–3056.
24. Iyer, G.; Michalet, X.; Chang, Y.-P.; Pinaud, F. F.; Matyas, S. E.; Payne, G.; Weiss, S. High Affinity scFv-Hapten Pair as a Tool for Quantum Dot Labeling and Tracking of Single Proteins in Live Cells. *Nano Lett.* **2008**, *8*, 4618–4623.
25. Roullier, V.; Clarke, S.; You, C.; Pinaud, F.; Gouzer, G. R.; Schaible, D.; Marchi-Artzner, V. R.; Piehler, J.; Dahan, M. High-Affinity Labeling and Tracking of Individual Histidine-Tagged Proteins in Live Cells Using Ni^{2+} Tris-Nitrilotriacetic Acid Quantum Dot Conjugates. *Nano Lett.* **2009**, *9*, 1228–1234.
26. Los, G. V.; Encell, L. P.; McDougall, M. G.; Hartzell, D. D.; Karassina, N.; Zimprich, C.; Wood, M. G.; Learish, R.; Ohana, R. F.; Urh, M.; *et al.* HaloTag: A Novel Protein Labeling Technology for Cell Imaging and Protein Analysis. *ACS Chem. Biol.* **2008**, *3*, 373–382.
27. Liu, D. S.; Phipps, W. S.; Loh, K. H.; Howarth, M.; Ting, A. Y. Quantum Dot Targeting with Lipoic Acid Ligase and HaloTag for Single-Molecule Imaging on Living Cells. *ACS Nano* **2012**, *6*, 11080–11087.
28. Howarth, M.; Takao, K.; Hayashi, Y.; Ting, A. Y. Targeting Quantum Dots To Surface Proteins In Living Cells with Biotin Ligase. *Proc. Natl. Acad. Sci. U.S.A.* **2005**, *102*, 7583–7588.
29. Chang, J. C.; Tomlinson, I. D.; Warnement, M. R.; Ustione, A.; Carneiro, A. M. D.; Piston, D. W.; Blakely, R. D.; Rosenthal, S. J. Single Molecule Analysis of Serotonin Transporter Regulation Using Antagonist-Conjugated Quantum Dots Reveals Restricted, p38 MAPK-Dependent Mobilization Underlying Uptake Activation. *J. Neurosci.* **2012**, *32*, 8919–8929.
30. Cutler, P. J.; Malik, M. D.; Liu, S.; Byars, J. M.; Lidke, D. S.; Lidke, K. A. Multi-Color Quantum Dot Tracking Using a High-Speed Hyperspectral Line-Scanning Microscope. *PLoS One* **2013**, *8*, e64320.
31. Gao, X.; Yang, L.; Petros, J. A.; Marshall, F. F.; Simons, J. W.; Nie, S. In Vivo Molecular and Cellular Imaging with Quantum Dots. *Curr. Opin. Biotechnol.* **2005**, *16*, 63–72.
32. Szent-Gyorgyi, C.; Schmidt, B. F.; Creeger, Y.; Fisher, G. W.; Zakel, K. L.; Adler, S.; Fitzpatrick, J. A.; Woolford, C. A.; Yan, Q.; Vasilev, K. V.; *et al.* Fluorogen-Activating Single-Chain Antibodies for Imaging Cell Surface Proteins. *Nat. Biotechnol.* **2008**, *26*, 235–240.
33. Vaughan, T. J.; Williams, A. J.; Pritchard, K.; Osbourn, J. K.; Pope, A. R.; Earnshaw, J. C.; McCafferty, J.; Hodits, R. A.; Wilton, J.; Johnson, K. S. Human Antibodies with Subnanomolar Affinities Isolated from a Large Non-immunized Phage Display Library. *Nat. Biotechnol.* **1996**, *14*, 309–314.
34. Szent-Gyorgyi, C.; Stanfield, R. L.; Andreko, S.; Dempsey, A.; Ahmed, M.; Capek, S.; Waggoner, A. S.; Wilson, I. A.; Bruchez, M. P. Malachite Green Mediates Homodimerization of Antibody VL Domains to Form a Fluorescent Ternary Complex with Singular Symmetric Interfaces. *J. Mol. Biol.* **2013**, *425*, 4595–4613.
35. Holleran, J.; Brown, D.; Fuhrman, M. H.; Adler, S. A.; Fisher, G. W.; Jarvik, J. W. Fluorogen-Activating Proteins as Biosensors of Cell-Surface Proteins in Living Cells. *Cytometry Part A* **2010**, *77A*, 776–782.
36. Goldman, E. R.; Balighian, E. D.; Mattoussi, H.; Kuno, M. K.; Mauro, J. M.; Tran, P. T.; Anderson, G. P. Avidin: A Natural Bridge for Quantum Dot-Antibody Conjugates. *J. Am. Chem. Soc.* **2002**, *124*, 6378–6382.
37. Grover, A.; Schmidt, B. F.; Salter, R. D.; Watkins, S. C.; Waggoner, A. S.; Bruchez, M. P. Genetically Encoded pH Sensor for Tracking Surface Proteins through Endocytosis. *Angew. Chem., Int. Ed.* **2012**, *51*, 4838−4842.
38. Parthasarathy, R. Rapid, Accurate Particle Tracking by Calculation of Radial Symmetry Centers. *Nat. Methods* **2012**, *9*, 724–726.
39. Saxton, M. J. Single-Particle Tracking: the Distribution of Diffusion Coefficients. *Biophys. J.* **1997**, *72*, 1744–1753.
40. Michalet, X. Mean Square Displacement Analysis of Single-Particle Trajectories with Localization Error: Brownian Motion in an Isotropic Medium. *Phys. Rev. E* **2010**, *82*, 041914.
41. Herrick-Davis, K.; Grinde, E.; Cowan, A.; Mazurkiewicz, J. E. Fluorescence Correlation Spectroscopy Analysis of Serotonin, Adrenergic, Muscarinic, and Dopamine Receptor Dimerization: The Oligomer Number Puzzle. *Mol. Pharmacol.* **2013**, *84*, 630–642.
42. Umemura, Y. M.; Vrljic, M.; Nishimura, S. Y.; Fujiwara, T. K.; Suzuki, K. G. N.; Kusumi, A. Both MHC Class II and Its GPI-Anchored Form Undergo Hop Diffusion as Observed by Single-Molecule Tracking. *Biophys. J.* **2008**, *95*, 435–450.
43. Cao, T. T.; Deacon, H. W.; Reczek, D.; Bretscher, A.; von Zastrow, M. A Kinase-Regulated PDZ-Domain Interaction Controls Endocytic Sorting of the β2-Adrenergic Receptor. *Nature* **1999**, *401*, 286–290.
44. Valentine, C. D.; Haggie, P. M. Confinement of Beta(1)- and Beta(2)-Adrenergic Receptors in the Plasma Membrane of Cardiomyocyte-Like H9c2 Cells Is Mediated by Selective Interactions with PDZ Domain and A-Kinase Anchoring Proteins but Not Caveolae. *Mol. Biol. Cell* **2011**, *22*, 2970–2982.
45. Yum, K.; Na, S.; Xiang, Y.; Wang, N.; Yu, M.-F. Mechanochemical Delivery and Dynamic Tracking of Fluorescent Quantum Dots in the Cytoplasm and Nucleus of Living Cells. *Nano Lett.* **2009**, *9*, 2193–2198.

46. Jing, C.; Cornish, V. W. A Fluorogenic TMP-Tag for High Signal-to-Background Intracellular Live Cell Imaging. *ACS Chem. Biol.* **2013**, *8*, 1704–1712.
47. Delehanty, J. B.; Mattoussi, H.; Medintz, I. L. Delivering Quantum Dots into Cells: Strategies, Progress and Remaining Issues. *Anal. Bioanal. Chem.* **2009**, *393*, 1091–1105.
48. Xu, J.; Teslaa, T.; Wu, T. H.; Chiou, P. Y.; Teitell, M. A.; Weiss, S. Nanoblade Delivery and Incorporation of Quantum Dot Conjugates into Tubulin Networks in Live Cells. *Nano Lett.* **2012**, *12*, 5669–5672.
49. Mittal, R.; Bruchez, M. P. Biotin-4-Fluorescein Based Fluorescence Quenching Assay for Determination of Biotin Binding Capacity of Streptavidin Conjugated Quantum Dots. *Bioconjugate Chem.* **2011**, *22*, 362–368.